

Supplementary Information

Common reactivity and properties of heme peroxidases: a DFT study of their origin

Daniel R. Ramos *, Paul G. Furtmüller, Christian Obinger, Ángeles Peña-Gallego, Ignacio Pérez-Juste, J. Arturo Santaballa *

Table S1. Relevant geometrical parameters for all studied species fully optimized at the B3LYP/cc-pVDZ computational level for all considered spin states. Distance (Å) between iron and imidazole nitrogen atom (Fe–Ni_i), the metal centre and either ferryl or water oxygen (Fe–O) or proton (Fe–H), and between ferryl oxygen and proton or hydrogen atom from the water molecule (O–H); mean distance (Å) between iron and the four pyrrole nitrogen atoms (Fe–N_p); and distance (Å) from Fe atom to heme pyrrole plane (Fe–pp). Positive values of the latter indicate displacement towards distal side, while negative figures stand for out-of-plane Fe placed at the opposite side. Bond orders are shown in parentheses, values under Fe–N_p account for total iron-pyrrole nitrogen bond order, *i.e.* the overall order of those four covalent bonds. Ni–Fe–O, Ni–Fe–H, and Fe–O–H stand for the angles (°) among these atoms.

Species	Spin	Fe–Ni _i	Fe–N _p	Fe–pp	Fe–O/H	O–H	Ni–Fe–O/H	Fe–O–H
Fe(III)-PO	1/2	1.924 (0.63)	1.997 (2.24)	-0.151				
	5/2	2.093 (0.33)	2.075 (1.52)	-0.391				
Fe(III)-PO-H ₂ O	1/2	1.948 (0.60)	2.012 (2.22)	-0.063	2.056 (0.39)		179.54	
	5/2	2.156 (0.32)	2.064 (1.47)	-0.139	2.304 (0.22)		179.25	
Fe(III)-PO-H	1/2	2.111 (0.39)	2.002 (2.05)	-0.100	1.493 (0.74)		179.67	
	5/2	2.093 (0.37)	2.070 (1.53)	-0.324	1.545 (0.50)		177.25	
Fe(II)-PO	0	1.974 (0.55)	2.022 (2.01)	-0.150				
	1	2.387 (0.21)	2.020 (1.90)	-0.103				
	2	2.213 (0.26)	2.103 (1.24)	-0.327				
Fe(II)-PO-H ₂ O	0	2.024 (0.49)	2.029 (2.00)	-0.059	2.123 (0.35)		179.28	
	1	2.395 (0.21)	2.021 (1.90)	-0.088	2.861 (0.11)		170.99	
	2	2.220 (0.26)	2.101 (1.23)	-0.295	2.907 (0.09)		169.51	
Fe(II)-PO-H	0	2.149 (0.37)	2.013 (2.07)	-0.048	1.483 (0.79)		179.79	
	1	2.136 (0.37)	2.011 (2.07)	-0.079	1.493 (0.76)		179.73	
	2	2.135 (0.35)	2.084 (1.36)	-0.169	1.507 (0.70)		179.93	
PO-I	1/2	2.149 (0.35)	2.023 (2.04)	0.091	1.630 (1.42)		179.80	
	5/2	2.152 (0.34)	2.085 (1.38)	0.126	1.627 (1.42)		179.77	
PO-I-H ₂ O	1/2	2.141 (0.36)	2.021 (2.06)	0.094	1.634 (1.39)	1.845 (0.04)	179.82	126.15
	5/2	2.144 (0.35)	2.083 (1.40)	0.127	1.631 (1.37)	1.875 (0.04)	179.81	124.56
PO-I-H	1/2	2.056 (0.45)	2.017 (2.00)	0.021	1.800 (0.91)	0.973 (0.76)	176.95	110.93
	5/2	2.160 (0.35)	2.059 (1.56)	0.089	1.810 (0.82)	0.973 (0.74)	178.52	112.79
PO-II	1	2.193 (0.32)	2.024 (2.09)	0.111	1.628 (1.44)		179.84	
	2	2.207 (0.30)	2.085 (1.43)	0.163	1.629 (1.42)		179.86	
PO-II-H ₂ O	1	2.178 (0.33)	2.022 (2.10)	0.112	1.634 (1.40)	1.798 (0.05)	179.62	121.73
	2	2.196 (0.31)	2.083 (1.44)	0.163	1.635 (1.37)	1.827 (0.05)	179.52	121.32
PO-II-H	1	2.069 (0.43)	2.025 (2.03)	0.030	1.807 (0.90)	0.972 (0.77)	178.06	109.19
	2	2.389 (0.22)	2.034 (1.86)	0.138	1.903 (0.63)	0.971 (0.77)	179.76	113.72

Table S2. Relevant geometrical parameters obtained experimentally for selected peroxidases: horseradish peroxidase (HRP), cytochrome c peroxidase (CCP), ascorbate peroxidase (APX), lactoperoxidase (LPO), and myeloperoxidase (MPO). Distance (\AA) between iron and imidazole nitrogen atom (Fe–N_i), the metal centre and either ferryl or water oxygen (Fe–O), and between ferryl oxygen and its proton (O–H); mean distance (\AA) between iron and the four pyrrole nitrogen atoms (Fe–N_p); and distance (\AA) from Fe atom to heme pyrrole plane (Fe–pp). Positive values of the latter indicate displacement towards distal side, while negative figures stand for out-of-plane Fe placed at the opposite side. N_i–Fe–O and Fe–O–H stand for the angles ($^{\circ}$) among these atoms.

Species	Peroxidase	PDB	Fe–N _i	Fe–N _p	Fe–pp	Fe–O	O–H	N _i –Fe–O	Fe–O–H
Ferric	HRP	1W4W ^a	2.093	2.021	−0.140	—	—	—	—
	CCP	1ZBY ^b	2.107	2.039	−0.274	2.330	—	176.15	
	CCP*	4CVI ^c	2.024	2.055	−0.181	2.651	—	169.64	
	APX	1OAG ^d	2.018	2.038	−0.199	1.944	—	176.90	
	LPO	2GJ1 ^e	2.145	2.051	−0.203	—	—	—	
	MPO	1CXP ^f	2.187	1.989	−0.321	2.899	—	178.06	
			2.189	1.986	−0.342	3.000	—	172.99	
Ferrous	HRP	1H58 ^g	2.133	2.028	−0.245	—	—	—	—
	CCP	2XJ8 ^h	2.062	2.117	−0.253	2.017	—	175.54	
	APX	2XJ6 ^h	2.013	2.104	−0.220	2.306	—	177.77	
Compound I	HRP	1HCH ^g	2.141	2.009	0.028	1.705	—	177.05	
	CCP	2XIL ^h	2.099	2.050	0.077	1.635	—	178.92	
	CCP*	4CVJ ^c	2.124	2.039	0.098	1.645	—	169.51	
	APX	2XI6 ^h	2.033	2.092	−0.087	1.743	—	176.11	
Compound II	HRP	1H55 ^g	2.140	2.007	0.003	1.839	—	176.41	
	CCP	2XJ5 ^h	2.121	2.070	−0.061	1.834	—	178.65	
	APX	2XIF ^h	1.994	2.027	−0.134	1.830	—	178.12	
	APX*	5JPR ⁱ	1.970	2.006	−0.081	1.879	0.986	178.76	142.28

* Structures obtained by neutron diffraction. ^a Ref. 73. ^b Ref. 22. ^c Ref. 27. ^d Ref. 74. ^e Ref. 75. ^f Ref. 76. ^g Ref. 72. ^h Ref. 14.

ⁱ Ref. 28.

Table S3. Mulliken atomic charges (a.u.) on relevant atoms obtained at the B3LYP/cc-pVDZ computational level. N_i , N_p , O_{Fe} , and Por refer to imidazole nitrogen, total charge on the four pyrrole nitrogens, ferryl oxygen, and porphine, respectively.

Species	Spin	Fe	N_i	N_p	O_{Fe}	H	Por	H_2O
Fe(III)-PO	1/2	0.64	-0.26	-1.63			-0.06	
	5/2	0.89	-0.35	-1.87			-0.23	
Fe(III)-PO-H ₂ O	1/2	0.32	-0.23	-1.43			-0.11	0.33
	5/2	0.66	-0.28	-1.76			-0.25	0.24
Fe(III)-PO-H	1/2	0.21	-0.26	-1.35		0.11	1.34	
	5/2	0.54	-0.35	-1.74		0.32	0.79	
Fe(II)-PO	0	0.34	-0.23	-1.39			-0.63	
	1	0.43	-0.21	-1.57			-0.62	
	2	0.59	-0.28	-1.68			-0.82	
Fe(II)-PO-H ₂ O	0	0.11	-0.19	-1.26			-0.66	0.25
	1	0.26	-0.20	-1.54			-0.59	0.13
	2	0.41	-0.26	-1.66			-0.77	0.10
Fe(II)-PO-H	0	0.18	-0.22	-1.38		0.05	0.46	
	1	0.32	-0.27	-1.50		0.13	0.24	
	2	0.17	-0.25	-1.34		0.07	0.45	
PO-I	1/2	0.29	-0.19	-1.28	-0.30		0.63	
	5/2	0.46	-0.20	-1.44	-0.30		0.44	
PO-I-H ₂ O	1/2	0.29	-0.18	-1.28	-0.35		0.66	0.00
	5/2	0.46	-0.19	-1.43	-0.34		0.47	0.00
PO-I-H	1/2	0.26	-0.21	-1.23	-0.32	0.19	1.44	
	5/2	0.40	-0.22	-1.35	-0.36	0.20	1.36	
PO-II	1	0.26	-0.18	-1.34	-0.34		-0.25	
	2	0.43	-0.18	-1.51	-0.35		-0.43	
PO-II-H ₂ O	1	0.26	-0.17	-1.33	-0.38		-0.20	-0.02
	2	0.42	-0.18	-1.49	-0.39		-0.38	-0.01
PO-II-H	1	0.22	-0.20	-1.25	-0.34	0.18	0.54	
	2	0.41	-0.22	-1.40	-0.43	0.17	0.58	

Table S4. Gibbs free energy obtained with B3LYP/cc-pVDZ ($T = 298.15$ K) for unprotonated species at ground spin state, and electron and proton published values employed in the study. Absolute values used as reference for data in Table 1.

Species	Spin	$\Delta G^\circ / \text{kJ mol}^{-1}$
e ⁻	1/2	-3.632 ^a
H ⁺	1/2 ^b	-1130.90 ^c
Fe(III)-PO	5/2	-3512299.76
Fe(II)-PO	2	-3512768.13
PO-I	1/2	-3709611.90
PO-II	1	-3710115.40
H ₂ O	0	-200643.65

^a Ref. 62. ^b Nuclear spin. ^c Refs. 59-61.

Table S5. Gibbs free energy values in kJ mol⁻¹ for the dissociation equilibrium of Fe(III)-PO-H₂O ($\Delta G^\circ_{\text{A}-\text{H}_2\text{O}(\text{aq})}$), and distance values (Å) between iron and water oxygen (Fe–O_w) obtained for the aqueous complex, corresponding bond orders are shown in parentheses. Data calculated by B3LYP and M06-2X functionals, with different basis sets for all atoms but Fe (LANL2DZ), and PCM at $T = 298.15$ K. The most favourable spin multiplicities were used; Fe(III)-PO with $S = 1/2$, and Fe(III)-PO-H₂O with $S = 1/2$ (B3LYP) or 5/2 (M06-2X).

B3LYP	$\Delta G^\circ_{\text{A}-\text{H}_2\text{O}(\text{aq})}$	Fe–O _w
6-31G(d,p)	-0.34	2.054 (0.38)
6-311G(2d,2p)	-7.29	2.068 (0.37)
6-311++G(2d,2p)	-31.29	2.070 (0.36)
cc-pVDZ	12.44	2.056 (0.39)
cc-pVTZ	-16.20	2.066 (0.36)
Aug-cc-pVTZ	-36.15	2.043 (0.37)
cc-pVQZ	-26.38	2.054 (0.37)
M06-2X	$\Delta G^\circ_{\text{A}-\text{H}_2\text{O}(\text{aq})}$	Fe–O _w
6-31G(d,p)	23.18	2.186 (0.23)
6-311G(2d,2p)	19.81	2.196 (0.22)
6-311++G(2d,2p)	2.35	2.201 (0.21)
cc-pVDZ	32.91	2.189 (0.24)
cc-pVTZ	8.46	2.194 (0.21)
Aug-cc-pVTZ	1.77	2.170 (0.21)
cc-pVQZ	3.18	2.178 (0.21)

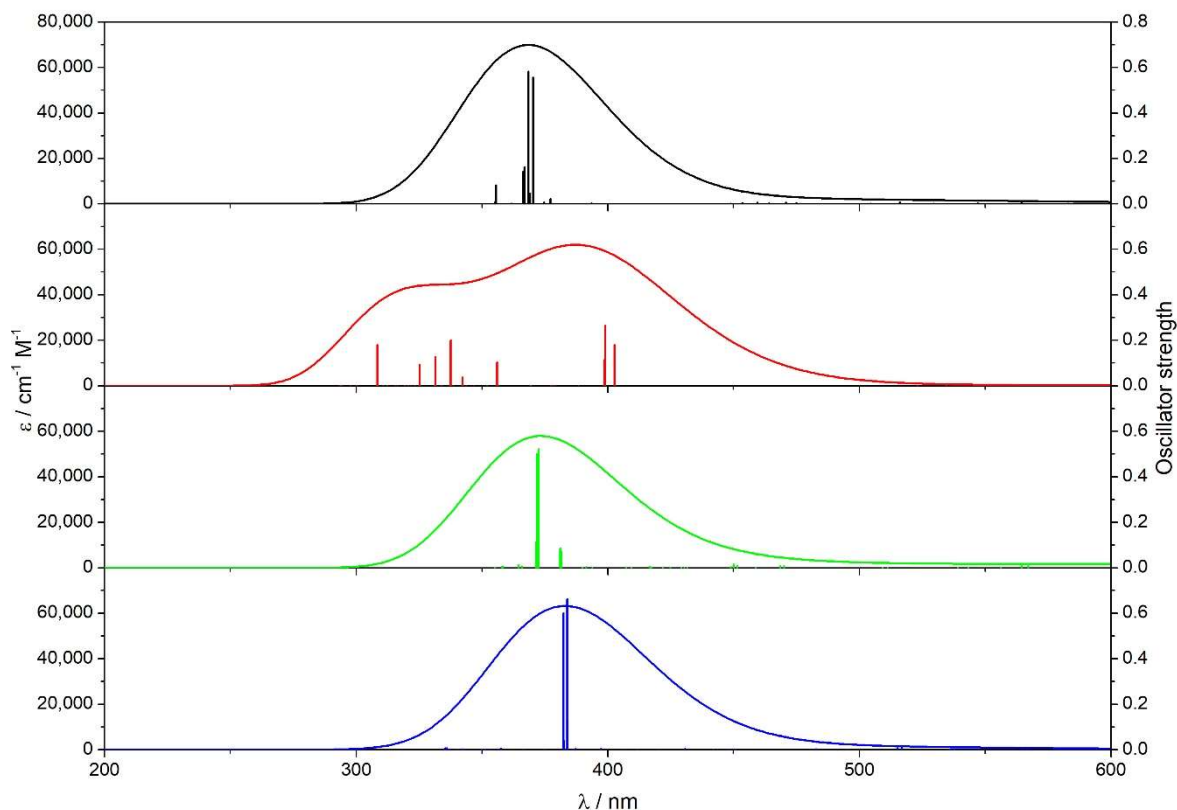
Table S6. p K_a values obtained for PO-I-H and PO-II-H through direct calculation (p K_a^1) and with the isodesmic method (p K_a^2). Data calculated by B3LYP and M06-2X functionals, with different basis sets for all atoms but Fe (LANL2DZ), and PCM at $T = 298.15$ K. The most favourable spin multiplicities were used; PO-I and PO-I-H with $S = 1/2$, and PO-II and PO-II-H with $S = 1$.

B3LYP	PO-I-H		PO-II-H	
	p K_a^1	p K_a^2	p K_a^1	p K_a^2
6-31G(d,p)	-1.9	-18.2	11.2	-5.1
6-311G(2d,2p)	-1.4	-14.1	8.8	-3.9
6-311++G(2d,2p)	-1.9	-9.0	8.2	1.0
cc-pVDZ	-4.2	-17.7	8.5	-5.0
cc-pVTZ	-1.3	-11.6	8.0	-2.3
Aug-cc-pVTZ	-1.5	-9.0	7.6	0.0
cc-pVQZ	-1.4	-10.1	7.7	-1.1
M06-2X	PO-I-H		PO-II-H	
	p K_a^1	p K_a^2	p K_a^1	p K_a^2
6-31G(d,p)	18.2	3.2	23.3	8.3
6-311G(2d,2p)	9.7	-2.3	22.4	10.5
6-311++G(2d,2p)	9.3	2.0	22.4	15.1
cc-pVDZ	16.2	3.4	21.0	8.2
cc-pVTZ	7.9	-1.4	21.3	12.0
Aug-cc-pVTZ	8.2	1.1	21.3	14.2
cc-pVQZ	8.7	0.5	21.4	13.2

Table S7. Wavelength (nm) and molar absorption coefficient ($\text{cm}^{-1}\cdot\text{mol}^{-1}\cdot\text{dm}^3$) of the Soret band obtained for all considered species and calculated with the B3LYP/cc-pVDZ computational method.

Species	Spin	λ	ϵ
Fe(III)-PO	5/2	368	69925
Fe(III)-PO-H ₂ O	1/2	372	71844
Fe(III)-PO-H	1/2	369	19822
Fe(II)-PO	2	387	61976
Fe(II)-PO-H ₂ O	2	388	59915
Fe(II)-PO-H	1	373	37872
PO-I	1/2	373	57952
PO-I-H ₂ O	1/2	375	51619
PO-I-H	1/2	400	3433
PO-II	1	383	63192
PO-II-H ₂ O	1	384	59793
PO-II-H	1	370	56965

Figure S1. Calculated excitation lines and the corresponding convoluted UV-vis absorption spectra at the Soret region obtained with the TD-DFT functional with the B3LYP/cc-pVDZ computational level at the most stable spin state for (A) non-protonated Fe(III)-PO (—), Fe(II)-PO (—), PO-I (—), and PO-II (—); (B) corresponding aquo complexes; and (C) protonated species.



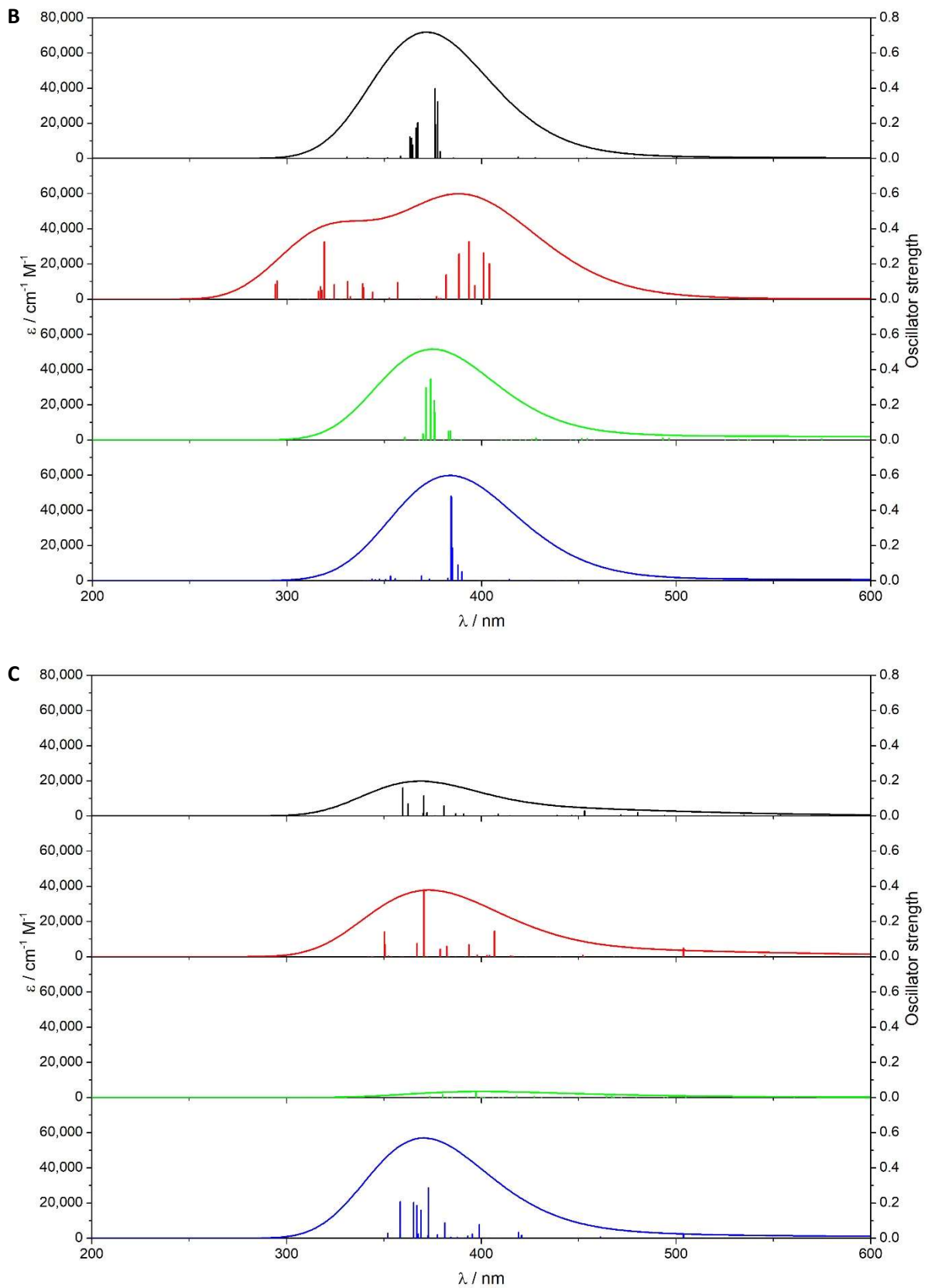


Table S8. Standard reduction potential (E°) values in mV relative to SHE calculated with direct and isodesmic methods, by B3LYP and M06-2X functionals, with different basis sets for all atoms but Fe (LANL2DZ), and PCM at $T = 298.15$ K. The most favourable spin multiplicities were used (as specified in parentheses).

	Redox couple					
	Fe(III)-PO/Fe(II)-PO (5/2 – 2)	PO-I/Fe(III)-PO (1/2 – 5/2)	PO-I/PO-II (1/2 – 1)	PO-I/PO-II-H (1/2 – 1)	PO-II/Fe(III)-PO (1 – 5/2)	PO-II-H/Fe(III)-PO (1 – 5/2)
Direct method						
B3LYP						
6-31G(d,p)	227	1136	592	1254	1679	1017
6-311G(2d,2p)	308	1279	825	1346	1733	1213
6-311++G(2d,2p)	365	1400	859	1345	1941	1456
cc-pVDZ	377	1066	741	1245	1391	886
cc-pVTZ	300	1324	859	1332	1790	1316
Aug-cc-pVTZ	121	1420	880	1328	1960	1512
cc-pVQZ	188	1388	876	1329	1900	1448
M06-2X						
6-31G(d,p)	652	2449	1403	2783	3496	2116
6-311G(2d,2p)	693	2328	1092	2419	3564	2236
6-311++G(2d,2p)	714	2452	1167	2490	3737	2414
cc-pVDZ	782	2405	1518	2761	3293	2050
cc-pVTZ	662	2358	1120	2380	3596	2336
Aug-cc-pVTZ	409	2468	1199	2461	3736	2475
cc-pVQZ	484	2443	1164	2431	3723	2456
Isodesmic method						
B3LYP						
6-31G(d,p)	17	858	382	1045	1470	807
6-311G(2d,2p)	-46	911	472	992	1380	860
6-311++G(2d,2p)	-110	1033	385	870	1467	982
cc-pVDZ	237	798	601	1105	1251	747
cc-pVTZ	-98	969	460	934	1392	918
Aug-cc-pVTZ	-373	1069	386	834	1466	1018
cc-pVQZ	-275	1036	414	867	1438	985
M06-2X						
6-31G(d,p)	-872	644	-121	1259	1973	593
6-311G(2d,2p)	-708	885	-310	1018	2162	834
6-311++G(2d,2p)	-812	939	-359	964	2211	888
cc-pVDZ	-698	621	39	1282	1813	570
cc-pVTZ	-770	955	-312	948	2164	904
Aug-cc-pVTZ	-1133	984	-342	919	2194	933
cc-pVQZ	-1033	989	-354	914	2206	938